c-Src Modulates Estrogen-Induced Stress and Apoptosis in Estrogen-Deprived Breast Cancer Cells

Ping Fan[1], Obi L. Griffith[2], Fadeke A. Agboke[1], Pavana Anur[4], Xiaojun Zou[1], Russell E. McDaniel[1], Karen Creswell[1], Sung Hoon Kim[3], John A. Katzenellenbogen[3], Joe W. Gray[2,4], and V. Craig Jordan[1]

Abstract

The emergence of anti-estrogen resistance in breast cancer is an important clinical phenomenon affecting long-term survival in this disease. Identifying factors that convey cell survival in this setting may guide improvements in treatment. Estrogen (E_2) can induce apoptosis in breast cancer cells that have been selected for survival after E_2 deprivation for long periods (MCF-7:5C cells), but the mechanisms underlying E_2-induced stress in this setting have not been elucidated. Here, we report that the c-Src kinase functions as a key adapter protein for the estrogen receptor (ER, *ESR1*) in its activation of stress responses induced by E_2 in MCF-7:5C cells. E_2 elevated phosphorylation of c-Src, which was blocked by 4-hydroxytamoxifen (4-OHT), suggesting that E_2 activated c-Src through the ER. We found that E_2 activated the sensors of the unfolded protein response (UPR), IRE1α (*ERN1*) and PERK kinase (*EIF2AK3*), the latter of which phosphorylates eukaryotic translation initiation factor-2α (eIF2α). E_2 also dramatically increased reactive oxygen species production and upregulated expression of heme oxygenase HO-1 (*HMOX1*), an indicator of oxidative stress, along with the central energy sensor kinase AMPK (*PRKAA2*). Pharmacologic or RNA interference–mediated inhibition of c-Src abolished the phosphorylation of eIF2α and AMPK, blocked E_2-induced ROS production, and inhibited E_2-induced apoptosis. Together, our results establish that c-Src kinase mediates stresses generated by E_2 in long-term E_2-deprived cells that trigger apoptosis. This work offers a mechanistic rationale for a new approach in the treatment of endocrine-resistant breast cancer. *Cancer Res; 73(14); 4510–20. ©2013 AACR.*

Introduction

Developing drugs that target the estrogen receptor (ER) either directly (tamoxifen) or indirectly (aromatase inhibitors) has improved the prognosis of breast cancer (1, 2). Although aromatase inhibitors show considerable advantages over tamoxifen with respect to patient disease-free survival and tolerability, acquisition of resistance to all forms of endocrine treatments is inevitable (3, 4). Multiple mechanistic changes are involved in antihormone resistance, which provides the scientific rationale for the clinical development of additional targeted therapies (5, 6). It is well-known that the biologic actions of E_2 are mediated through the ER, which functions in the nucleus as ligand-dependent transcription factors to promote gene transcription and stimulation of cell growth (7). Paradoxically, laboratory evidence shows that E_2 can induce apoptosis in sensitive antihormone-resistant cells *in vivo* (8–10). This new targeted strategy provides novel therapeutic approaches to endocrine-resistant breast cancer. A recent phase II clinical trial reports that E_2 provides a clinical benefit for patients with aromatase inhibitor–resistant advanced breast cancer (11). In addition, the laboratory results on E_2 -induced apoptosis using antihormone-treated MCF-7 cells have been used to explain the reduction of breast cancer and the reduction in mortality observed in postmenopausal hysterectomized women in their 60s treated with conjugated equine estrogen (CEE) when compared with a placebo-treated control (12). The antitumor action of CEE is observed, not only during CEE treatment but also for 6 years after treatment. These data suggest a cidal effect for CEE and has been noted recently (13). These encouraging clinical results prompted us to investigate the mechanisms underlying E_2-induced apoptosis to increase the therapeutic benefits of E_2 in aromatase inhibitor–resistant breast cancer.

Experimental evidence has established the oncogene, c-Src, as a critical component of multiple signaling pathways that regulate proliferation, survival, angiogenesis, and metastasis (14, 15). Increased c-Src activity is believed to play an important role in the development and progression of breast cancer

Authors' Affiliations: [1]Department of Oncology, Lombardi Comprehensive Cancer Center, Georgetown University, Washington, District of Columbia; [2]Lawrence Berkeley National Laboratory, Life Sciences Division, Cancer & DNA Damage Responses, Berkeley, California; [3]Department of Chemistry, University of Illinois at Urbana-Champaign, Urbana, Illinois; and [4]Biomedical Engineering Department, Oregon Health and Science University, Portland, Oregon

Note: Supplementary data for this article are available at Cancer Research Online (http://cancerres.aacrjournals.org/).

Current address for O.L. Griffith: Department of Medicine, Division of Oncology, The Genome Institute, Washington University, St. Louis, MO.

Corresponding Author: V. Craig Jordan, Scientific Director of Lombardi Comprehensive Cancer Center, Georgetown University, E507A Research Bldg, 3970 Reservoir RD NW, Washington, DC 20057. Phone: 202-687-2897; Fax: 202-687-6402; E-mail: vcj2@georgetown.edu

doi: 10.1158/0008-5472.CAN-12-4152

(16), and c-Src has been considered as a survival signal for endocrine resistant breast cancer cells (17). Therefore, a c-Src inhibitor administered as a single-agent or in combination with other antihormone therapy has the potential to enhance the inhibitory effects of antihormones and delay antihormone resistance (18). These observations highlight c-Src as an important therapeutic target for the treatment of human breast cancer.

Mitochondria are important intracellular organelles involved in apoptosis via an intrinsic pathway (19). Although the molecular mechanisms of E_2-induced apoptosis are not fully understood, evidence indicates that mitochondria-related caspase pathways are involved (20, 21). Similarly, a variety of events in apoptosis focus on mitochondria, including the loss of mitochondrial transmembrane potential, release of cytochrome *c*, and participation of pro- and antiapoptotic Bcl-2 family proteins (22, 23). However, accumulating evidence suggests that the endoplasmic reticulum where members of the Bcl-2 family of proteins localize is also a major point of integration of pro-apoptotic signaling or damage sensing (24, 25). The endoplasmic reticulum senses local stress such as unfolded protein (UPR) through a set of pathways known as the UPR (26), which activates 3 transmembrane sensors PRK-like endoplasmic reticulum kinase (PERK), inositol-requiring 1 alpha (IRE-1α), and activating transcription factor 6 (ATF-6) in endoplasmic reticulum (26). Depending on the duration and degree of stress, the UPR can provide either survival signals by activating adaptive and antiapoptotic signals or death signals by inducing cell death programs (27, 28).

We have found that E_2 changes the cell number according to the treatment period in long-term E_2-deprived breast cancer cell lines MCF-7:5C and MCF-7:2A (25). E_2 has the capacity to decrease around 80% of cell number in MCF-7:5C cells after 7 days treatment, whereas in MCF-7:2A cells after 2-week treatment (29). Unexpectedly, the c-Src inhibitor effectively rescues the decreasing of cell number by E_2 in 2 long-term E_2-deprived cell lines (29). The goal of this study is to identify the mechanisms underlying the early stage of E_2-induced apoptosis and the function of c-Src in the process of E_2-initiated apoptosis. To that end, we show that E_2 triggers endoplasmic reticulum stress and oxidative stress, which activate 2 main apoptotic pathways, the mitochondrial (intrinsic) and death receptor (extrinsic) pathways, whereas c-Src plays an essential role in mediating stress responses induced by E_2 in MCF-7:5C cells. These findings have important clinical implications for the appropriate application of combination therapies in advanced aromatase inhibitor–resistant breast cancer.

Materials and Methods

Materials

Estradiol was purchased from Sigma-Aldrich. c-Src inhibitor PP2 was purchased from CalBiochem. ERα antibody was from Santa Cruz Biotechnology. Total mitogen-activated protein kinase (MAPK), phosphorylated MAPK, phosphorylated c-Src, phosphorylated eIF2α, total eIF2α, and IRE1α antibodies were from Cell Signaling Technology. Total c-Src mouse antibody was from Millipore. Estrogen dendrimer conjugate (EDC) was a kind gift by Dr. J.A. Katzenellenbogen (University of Illinois at Urbana-Champaign, Urbana, IL).

Cell culture conditions and cell proliferation assays

Estrogen-deprived MCF-7:5C cells were maintained in estrogen-free RPMI-1640 medium supplemented with 10% dextran-coated charcoal-stripped FBS as previously described (20). The DNA fingerprinting pattern of cell line is consistent with the report by the American Type Culture Collection (29). The DNA content of the cells, a measure of proliferation, was determined by using a DNA fluorescence quantitation kit (29).

Cell-cycle analysis

Briefly, MCF-7:5C cells were treated with vehicle (0.1% EtOH) and E_2 (10^{-9} mol/L), respectively. Cells were harvested and gradually fixed with 75% EtOH on ice. After staining with propidium iodide (PI), cells were analyzed using a FACSort flow cytometer (Becton Dickinson), and the data were analyzed with ModFit software.

Annexin V analysis of apoptosis

The FITC Annexin V Detection Kit I (BD Pharmingen) was used to quantify apoptosis by flow cytometry according to the manufacturer's instructions. In brief, MCF-7:5C cells were treated with different compounds, respectively. Cells were suspended in 1× binding buffer and 1×10^5 cells were stained simultaneously with fluorescein isothiocyanate (FITC)-labeled Annexin V (FL1-H) and PI (FL2-H). Cells were analyzed using FACSort flow cytometer (Becton Dickinson).

Mitochondrial/TRANSMEMBRANE potential ($\Delta\psi_m$) detection

Mitochondrial membrane potential was measured by flow cytometry using the cationic lipophilic green fluorochrome rhodamine-123 (Rh123; Molecular Probes) as previously described (20). Disruption of $\Delta\psi_m$ is associated with a lack of Rh123 retention and a decrease in fluorescence.

Detection of oxidative stress

Intracellular reactive oxygen species (ROS) were detected by fluorescent dye 2′,7′-dichlorofluorescein diacetate (H_2DCFDA, Invitrogen; ref. 30). Briefly, MCF-7:5C cells were treated with E_2 for different time points using vehicle (0.1% EtOH) cells as control. Cells were loaded with 1 μmol/L CM-H_2DCFDA for 10 minutes and washed with PBS twice. Then, cells were monitored at fluorescence 530 nm and an excitation wavelength of 488 nm through flow cytometry.

Immunoblotting

Proteins were extracted in cell lysis buffer (Cell Signaling Technology) supplemented with Protease Inhibitor Cocktail (Roche) and Phosphatase Inhibitor Cocktail Set I and Set II (Calbiochem). The immunoblotting was conducted as previously described (29).

Transient transfection reporter gene assays

Transient transfection assay was conducted using a dual-luciferase system (Promega). To determine ER transcriptional

activity, cells were transfected with an estrogen response element (ERE)-regulated (pERE (5×) TA-ffLuc plus pTA-srLuc) dual-luciferase reporter gene sets. The cells were treated with E_2 for 24 hours following the transfection. Then, the cells were harvested and processed for dual-luciferase reporter activity, in which the firefly luciferase activity was normalized by *Renilla* luciferase activity.

Quantitative real-time reverse transcription PCR

Total RNA, isolated with an RNeasy Micro Kit (Qiagen), was converted to first-strand cDNA using a kit from Applied Biosystems. Quantitative real-time PCR assays were done with the SYBR Green PCR Master Mixes (Applied Biosystems) and a 7900HT Fast Real-time PCR System (Applied Biosystems). All primers were synthesized in Integrated DNA Technologies. The sequence of primers is shown in the Supplementary Table S1. All the data were normalized by 36B4.

RNA sequencing analysis

MCF-7:5C cells were treated with different compounds for 72 hours. Cells were harvested in TRIzol. Total RNA was isolated with an RNeasy Micro Kit. These long RNA samples were first converted into a library of cDNA fragments. Sequencing adaptors were subsequently added to each cDNA fragment and a 2×100 bp paired-end sequence was obtained from each cDNA using high-throughput sequencing technology (Illumina GAII). An average of 73.8 million such reads was produced for each sample. The resulting sequence reads were aligned to reference genome build hg19 using TopHat 1.3.0 (31), a splice junction aligner. Transcript abundance was estimated as Fragments Per Kilobase of exon per Million fragments mapped (FPKM), using Cufflinks 1.0.3 (32). Additional analysis was conducted with the alternative expression analysis by sequencing (Alexa-seq) software package as previously described (33). Gene expression measures were compared between Cufflinks and Alexa-seq for the set of 17,993 overlapping genes. Correlations were excellent with Spearman correlations of 0.955 to 0.971 for the 6 samples. Pathway analysis was conducted with DAVID (34) on lists of differentially expressed gene lists.

Statistical analysis

All reported values are the means ± SE. Statistical comparisons were determined with 2-tailed Student *t* tests. Results were considered statistically significant if the $P < 0.05$.

Results

c-Src mediated estrogen-activated growth pathways in long-term estrogen-deprived breast cancer cells MCF-7:5C

It is well-documented that E_2 stimulates growth and prevents apoptosis in wild-type breast cancer cells and estrogen-responsive osteoblast cells (35, 36). In contrast, physiologic concentrations of E_2 induce apoptosis in long-term E_2-deprived breast cancer cells (20, 21). c-Src plays a critical role in relaying ER signaling pathways in breast cancer cells (37). To investigate the function of E_2 and c-Src in long-term E_2-deprived breast cancer cells MCF-7:5C, a specific c-Src tyrosine kinase inhibitor, PP2, was used to block phosphorylation of c-Src (Fig. 1A). It also effectively abolished the growth pathways including the MAPK and phosphoinositide 3-kinase (PI3K)/AKT pathways in MCF-7:5C cells (Fig. 1A). E_2 activated c-Src through ER as 4-hydroxytamoxifen (4-OHT) completely suppressed phosphorylation of c-Src (Fig. 1B). Although our previous finding showed that E_2 initiates apoptosis in MCF-7:5C cells (20), E_2 was able to activate nongenomic (Supplementary Fig. S1A) and genomic pathways in MCF-7:5C cells (Fig. 1C). These actions were blocked by the c-Src inhibitor, PP2 (Fig. 1C and Supplementary Fig. S1A). Even though the characteristic E_2-induced apoptosis occurs after 72-hour treatment (20), cell numbers were initially increased by E_2 with a high percentage in S-phase (Fig. 1D). All of these results suggested that E_2 caused an imbalance between growth and apoptosis in MCF-7:5C cells.

Inhibition of c-Src suppressed estrogen-induced apoptosis in MCF-7:5C cells

We have shown that long-term E_2 deprivation increases c-Src activity (29). Therefore, we addressed the question of whether the c-Src inhibitor, PP2, in combination with E_2 would enhance apoptosis in MCF-7:5C cells. Unexpectedly, the c-Src inhibitor blocked apoptosis initiated by E_2 (Fig. 2A and Supplementary Fig. S1D). To confirm that inhibition of c-Src could block E_2-induced apoptosis, a specific siRNA was used to knock down c-Src in MCF-7:5C cells (Fig. 2B), which reduced the percentage of Annexin V binding induced by E_2 (Fig. 2C). Further experiments showed that E_2 disrupted mitochondrial membrane potential ($\Delta\psi_m$) after 48-hour treatment, which was measured by flow cytometry using Rh123 (Fig. 2D). The c-Src inhibitor PP2 and 4-OHT both prevented reduction of Rh123 retention induced by E_2 (Fig. 2D). These data showed that E_2-triggered apoptosis use the c-Src tyrosine kinase pathway. To evaluate the role of the nongenomic pathway in E_2-induced apoptosis, studies were completed with a synthetic ligand, EDC, that only activates the nongenomic pathway at certain concentration (38). The results showed that EDC (10^{-8} mol/L) activated the nongenomic pathway incorporating c-Src (Supplementary Fig. S2). Importantly, EDC had no capacity to activate endogenous E_2 target gene pS2 and did not induce apoptosis in MCF-7:5C cells (Supplementary Fig. S2). All of these findings suggested that the nongenomic pathway does not play a critical role in triggering E_2-induced apoptosis.

Suppression of E_2-induced apoptosis by the c-Src inhibitor was independent of the classical ERE-regulated transcriptional genes in MCF-7:5C cells

The ER is the initial site for E_2 to induce apoptosis as antiestrogens ICI 182,780 and 4-OHT completely block apoptosis triggered by E_2 (ref. 20 and Supplementary Fig. S3A). In addition to the mediation of ER growth pathways, c-Src is involved in the process of ligand-activated ER ubiquitylation (39). Therefore, blockade of c-Src tyrosine kinase with PP2 further increased ERα protein and mRNA expression levels in MCF-7:5C cells (Fig. 3A). E_2 activated ERE activity, which could be blocked by 4-OHT but not by PP2 (Fig. 3B). It was interesting to find that the c-Src inhibitor alone could upregulate

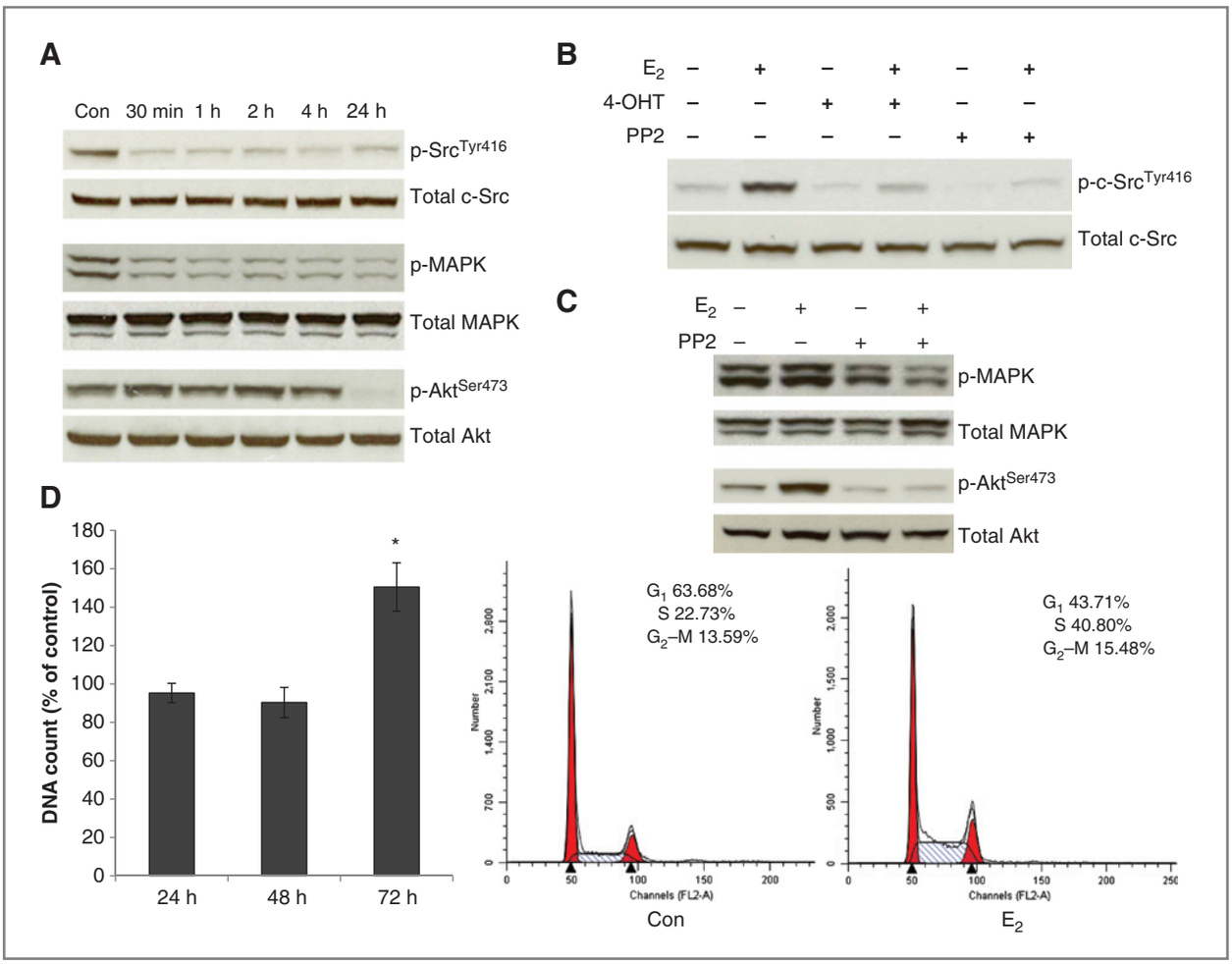

Figure 1. c-Src mediated estrogen-activated growth pathways in MCF-7:5C cells. A, MCF-7:5C cells were treated with vehicle (0.1% dimethyl sulfoxide) and PP2 (5×10^{-6} mol/L) for different durations. Phosphorylated c-Src, MAPK, and Akt were detected by immunoblotting. Total c-Src, MAPK, and Akt were used for loading controls. B, MCF-7:5C cells were treated with vehicle (0.1% dimethyl sulfoxide), E_2 (10^{-9} mol/L), 4-OHT (10^{-6} mol/L), E_2 (10^{-9} mol/L) plus 4-OHT (10^{-6} mol/L), PP2 (5×10^{-6} mol/L), E_2 (10^{-9} mol/L) plus PP2 (5×10^{-6} mol/L), respectively for 48 hours. Phosphorylated c-Src was detected by immunoblotting. Total c-Src was used for loading control. C, MCF-7:5C cells were treated with E_2 or combined with PP2, respectively, for 24 hours. Phosphorylated MAPK and Akt were examined by immunoblotting. Total MAPK and Akt were used for loading controls. D, MCF-7:5C cells were treated with vehicle and E_2 for different durations. Total DNA was determined using a DNA fluorescence quantitation kit. As a parallel experiment, MCF-7:5C cells were treated with vehicle and E_2 for 72 hours. Cells were fixed for cell-cycle analysis. *, $P < 0.05$, compared with respective control.

E_2-inducible gene pS2 and was additive with E_2 to elevate pS2 mRNA level (Fig. 3C). Another important ER target gene progesterone receptor (PR) has been regarded as an indicator of a functional ER pathway, as expression of PR is regulated by E_2. Although the c-Src inhibitor alone did not elevate PR expression, it dramatically synergized with E_2 to upregulate PR mRNA (Fig. 3D). All of these results showed that blockade of c-Src increased expression of classical ER target genes. It also implied that classical ER pathway might not directly involve in the E_2-induced apoptosis.

c-Src was involved in the process of triggering apoptosis-related genes by E_2 in MCF-7:5C cells

To further investigate the mechanisms of the suppression of E_2-induced apoptosis by PP2, RNA-seq analysis was conducted to examine the genes regulated by E_2 to trigger apoptosis in MCF-7:5C cells. A wide range of apoptosis-related genes was activated by E_2 (Fig. 4A), which were functionally classified into 3 groups: *TP53*-related genes (such as *TP63*, *PMAIP1*, and *CYFIP2*), stress-related genes (such as *HMOX1*, *PPP1R15A*, *ZAK*, *NUAK2*, etc.), and inflammatory response–related genes (such as *LTB*, *FAS*, *TNFRSF21*, *CXCR4*, etc.). Most were stress-related genes (Supplementary Fig. S3B). Consistent with the biologic experiments, 4-OHT and PP2 both blocked apoptosis-related genes induced by E_2 but to a different extent in MCF-7:5C cells (Fig. 4A). The majority of these apoptosis-related genes were confirmed by real-time PCR with similar changes noted as in RNA-seq analysis (Fig. 4B–D and Supplementary Fig. S4). E_2 dramatically increased p63 mRNA levels (Fig. 4B) but did not arrest cells in the G_1 phase. In fact, S-phase was markedly elevated in MCF-7:5C cells (Fig. 1D). Heme oxygenase 1 (*HMOX1*), which is active at high concentrations of heme,

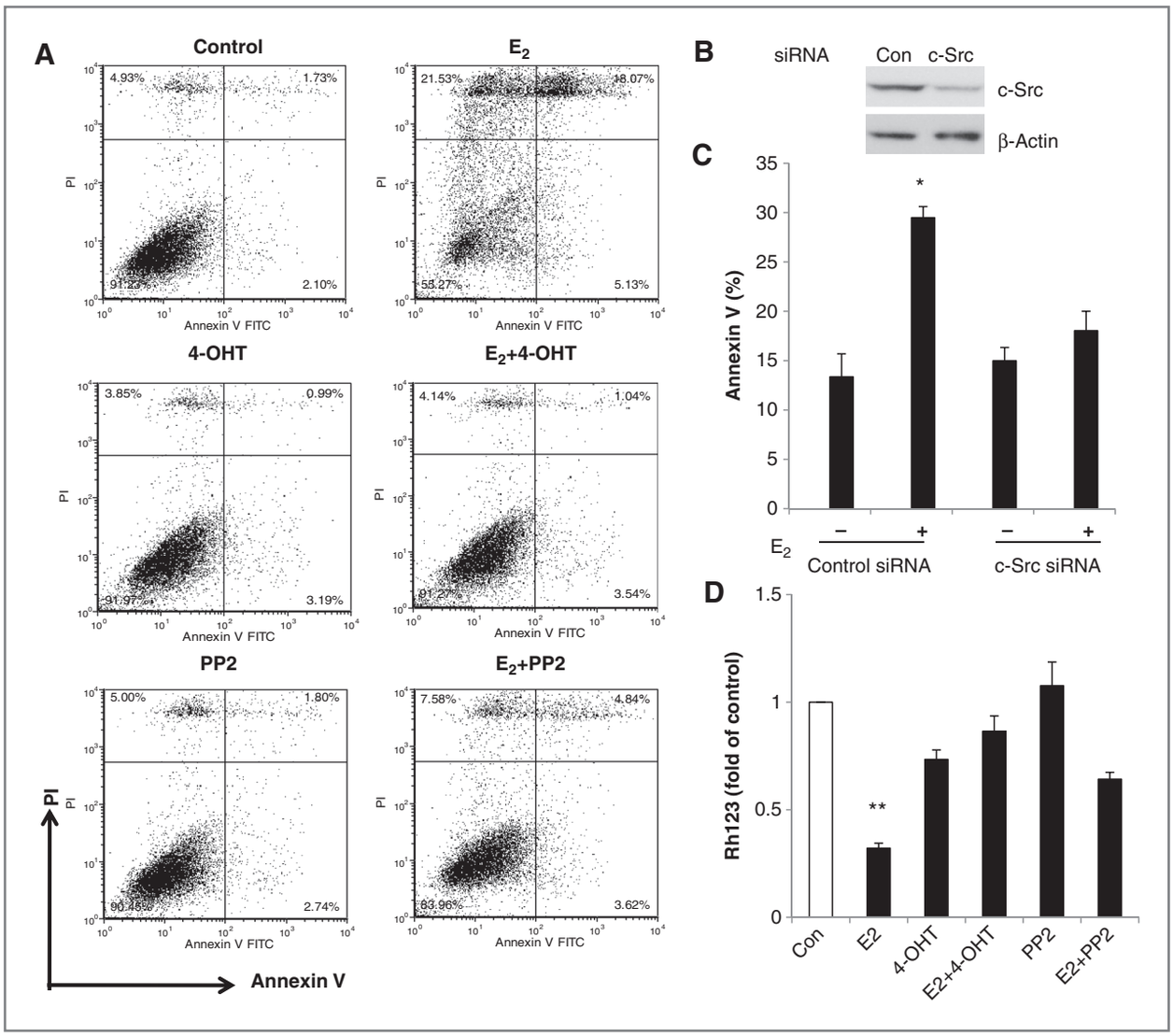

Figure 2. Inhibition of c-Src suppressed estrogen-induced apoptosis in MCF-7:5C cells. A, MCF-7:5C cells were treated with different compounds respectively as above for 72 hours and Annexin V binding assay was used to detect apoptosis. B, MCF-7:5C cells were transfected with siRNA of c-Src for 72 hours using nontarget siRNA as control. c-Src was detected by immunoblotting. The β-actin was used for loading control. C, MCF-7:5C cells were transfected with c-Src siRNA and nontarget siRNA as above. Then, they were treated with vehicle (0.1% EtOH) and E_2 (10^{-9} mol/L), respectively, for 72 hours. Apoptosis was detected through Annexin V binding assay. *, $P < 0.05$, compared with control. D, MCF-7:5C cells were treated with different compounds respectively as above for 48 hours and cells were harvested to detect mitochondrial potential through Rh123. **, $P < 0.001$, compared with control.

catalyzes the degradation of heme and is thought to function as an oxidative stress indicator (40). In breast cancer cells, cytochrome *c* is a major source of heme protein found in the inner membrane of the mitochondrion. E_2 markedly increased *HMOX1* in MCF-7:5C cells (Fig. 4C), thereby confirming that E_2 may damage the mitochondria and caused cytochrome *c* release. In contrast to MCF-7:5C cells, E_2 decreased *HMOX1* levels in wild-type MCF-7 cells (Supplementary Fig. S5A) and clearly did not change *HMOX1* expression in another long-term E_2-deprived cell line MCF-7:2A (Supplementary Fig. S5B), both of MCF-7 and MCF-7:2A do not undergo apoptosis after exposure to E_2 in the first 3 days. In addition, E_2 upregulated TNF family members (such as TNFα, LTA, and LTB), which were abolished by 4-OHT and PP2 (Fig. 4D and Supplementary Fig. S6A and S6B). Low dose of TNFα activated pro-apoptotic pathways in MCF-7:5C cells and inhibited cell growth (Supplementary Fig. S6C and S6D). All of these data suggested that E_2 widely activated intrinsic and extrinsic apoptosis pathways and c-Src was directly involved in mediating apoptosis.

The c-Src inhibitor blocked estrogen-induced oxidative stress in MCF-7:5C cells

ROSs are the product of oxidative stress by mitochondria, whereas an increase in ROS contributes to degenerative changes in mitochondrial function (41). Under physiologic conditions, cellular ROS levels are tightly controlled by

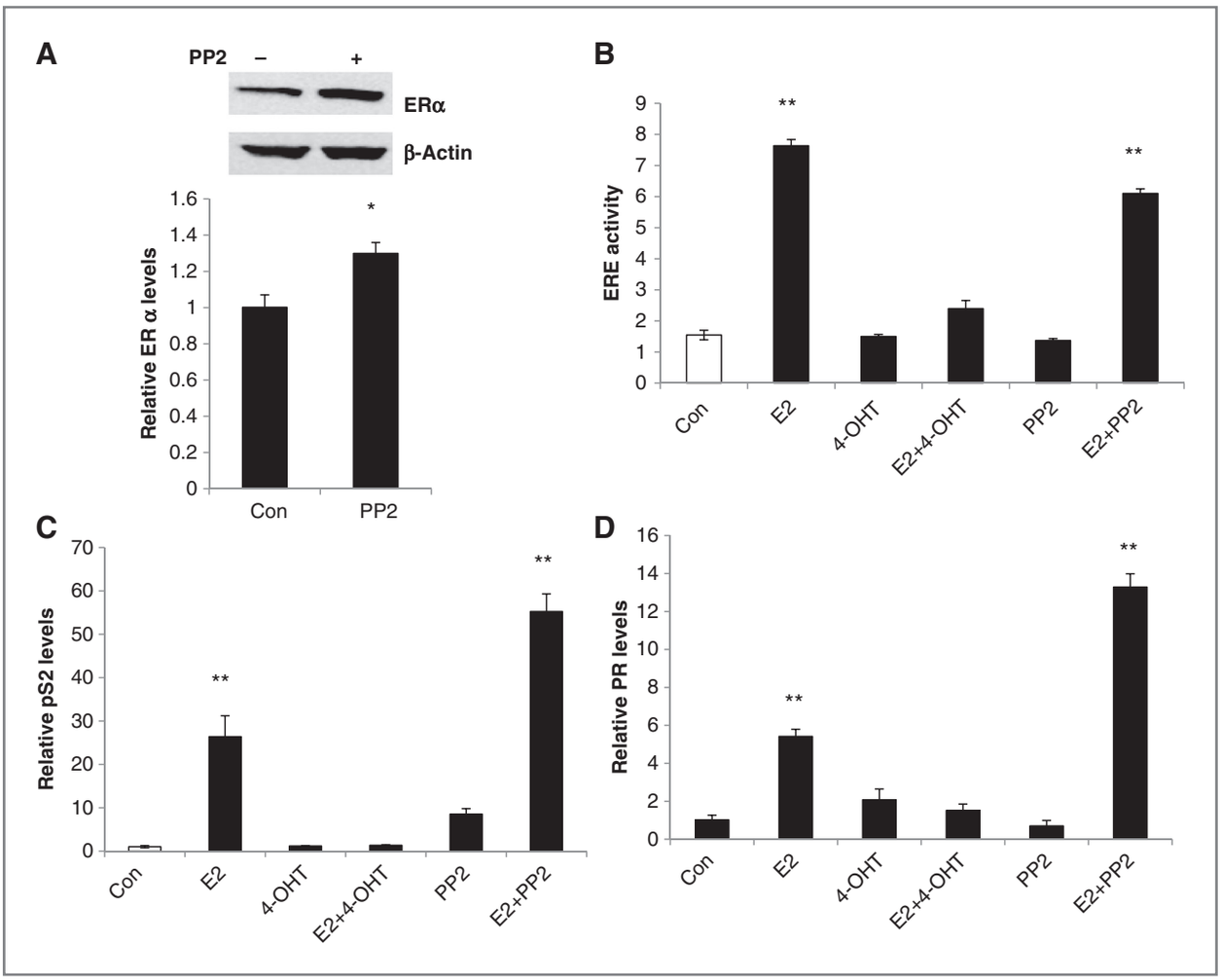

Figure 3. Suppression of E_2-induced apoptosis by the c-Src inhibitor was independent of the classical ERE-regulated transcriptional genes in MCF-7:5C cells. A, MCF-7:5C cells were treated with vehicle (0.1% dimethyl sulfoxide) and PP2 (5×10^{-6} mol/L), respectively, for 24 hours. ERα protein was detected by immunoblotting. ERα mRNA was quantified with quantitative PCR (qPCR). *, $P < 0.05$, compared with control. B, MCF-7:5C cells were transfected with ERE firefly luciferase plasmid plus *Renilla* luciferase plasmid. Then, cells were treated with different compounds respectively for 24 hours to detect ERE activity. **, $P < 0.001$, compared with control. C, MCF-7:5C cells were treated with different compounds respectively for 24 hours. The pS2 mRNA was quantified with qPCR. **, $P < 0.001$, compared with control. D, MCF-7:5C cells were treated with different compounds respectively for 72 hours. The PR mRNA was quantified with qPCR. **, $P < 0.001$, compared with control.

low-molecular-weight radical scavengers and by a complex intracellular network of enzymes such as catalases (*CAT*) and superoxide dismutases (*SOD*). Under conditions of lethal stress, ROSs are considered as key effectors of cell death (42). Intracellular ROSs were detected by CM-H_2DCFDA through flow cytometry (Fig. 5A). Detectable ROS appeared after 48 hours of treatment with E_2. The production of ROS reached a peak after 72-hour treatment (Fig. 5A and B). Blocking ER (by 4-OHT) and c-Src (by PP2) abolished ROS generation induced by E_2 (Fig. 5C), indicating that both ER and c-Src were upstream signals of ROS. Free-radical scavengers Mn-TBAP, catalase, and sodium formate (SF) that respectively act on superoxide radical (O_2^-), H_2O_2, and hydroxyl radical (OH^-) were used to suppress the production of ROS. Our results suggested that H_2O_2 and OH^- were the major sources of ROS induced by E_2. This conclusion was based on the observation that catalase and sodium formate inhibited E_2 -induced apoptosis, whereas Mn-TBAP was less effective (Fig. 5D). The RNA-seq analysis showed that E_2 did not significantly regulate antioxidant enzymes such as catalases (*CAT*) and superoxide dismutases (*SOD*) in MCF-7:5C cells (data not shown). Our results suggest that E_2 has the potential to damage mitochondria to cause oxidative stress.

c-Src was involved in estrogen-induced endoplasmic reticulum stress in MCF-7:5C cells

Our previous global gene array data show that E_2 activates genes related to endoplasmic reticulum stress in MCF-7:5C cells (25). To relieve stress, sensors of UPRs are activated as initial responses (43). In this study, a significant induction of UPR sensors, inositol-requiring protein 1 alpha (IRE1α) and PERK/eukaryotic translation initiation factor-2α (eIF2α), by E_2

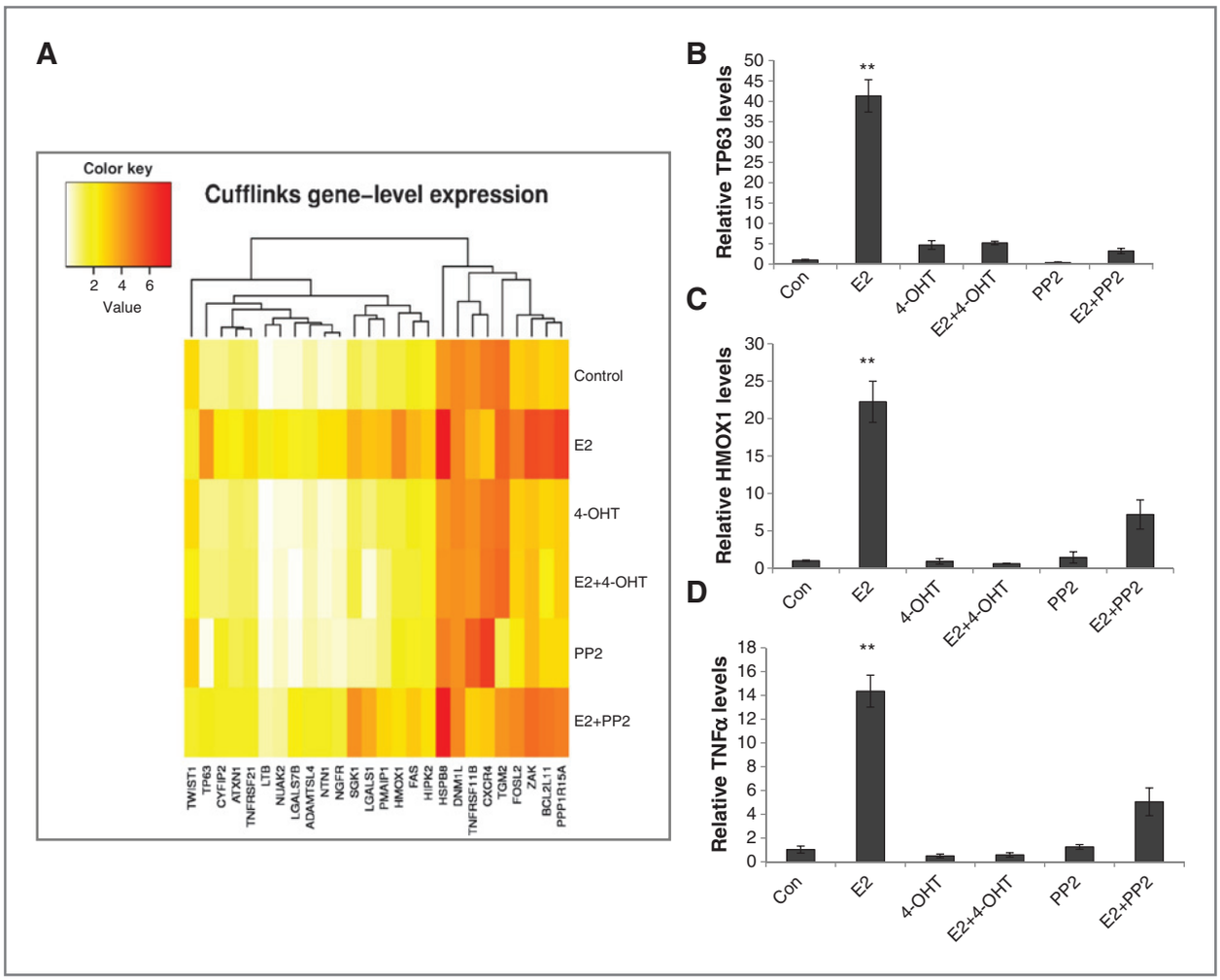

Figure 4. c-Src was involved in the process of triggering apoptosis-related genes by E_2 in MCF-7:5C cells. A, MCF-7:5C cells were treated with vehicle and different compounds respectively as above for 72 hours. Cells were harvested in TRIzol for RNA-seq analysis. B, MCF-7:5C cells were treated with different compounds as above. TP63 mRNA was quantified with quantitative PCR (qPCR). **, $P < 0.001$, compared with control. C, HMOX1 mRNA was quantified with qPCR. **, $P < 0.001$, compared with control. D, TNFα mRNA was quantified with qPCR. **, $P < 0.001$, compared with control.

occurred after 24 hours of treatment and was further increased by prolonging treatment times in MCF-7:5C cells (Fig. 6A). The anti-estrogen 4-OHT completely abolished the response (Fig. 6A). The PERK inhibitor blocked phosphorylation of eIF2α and prevented E_2-induced apoptosis (Fig. 6B and C), confirming that endoplasmic reticulum stress was important in the apoptosis initiated by E_2. Phosphorylated eIF2α closely associates with an important cellular energy sensor, adenosine monophosphate (AMP)-activated protein kinase (AMPK) to regulate protein translation and apoptosis (44). AMPK, which phosphorylates many metabolic enzymes to stimulate catabolic pathways and increases the capacity of cells to produce ATP (45), was significantly activated after 48-hour treatment with E_2 (Fig. 6D). The c-Src inhibitor, PP2, blocked the phosphorylation of eIF2α but not IRE1α induced by E_2 (Fig. 6E). PP2 also prevented the activation of AMPK after E_2 treatment (Fig. 6F). All of these data indicate that c-Src acts as an important transducer in the protein kinase pathways (eIF2α and AMPK) of stress response (Fig. 6E and F) that result in apoptosis.

Discussion

We have previously investigated the inhibitory effects of E_2 on long-term endocrine-resistant breast cancer tumor growth *in vivo* (8–10). And we have confirmed that this therapeutic effect is related with the apoptosis induced by E_2 (20). This scientific discovery has been used in the clinical trials to treat aromatase inhibitor–resistant patients with breast cancer and 30% of patients receive benefit (11). The potential limitation on translational research in the treatment of hormone-responsive breast cancer is that only 4 ER-positive breast cancer cell lines are available to use routinely (46). Only MCF-7 of the 4 produces the phenotype of E_2-induced apoptosis observed clinically (20, 21). The purpose of establishing long-term E_2 deprivation *in vitro* models is to mimic administration of an aromatase inhibitor that reduces levels of circulating estrogen

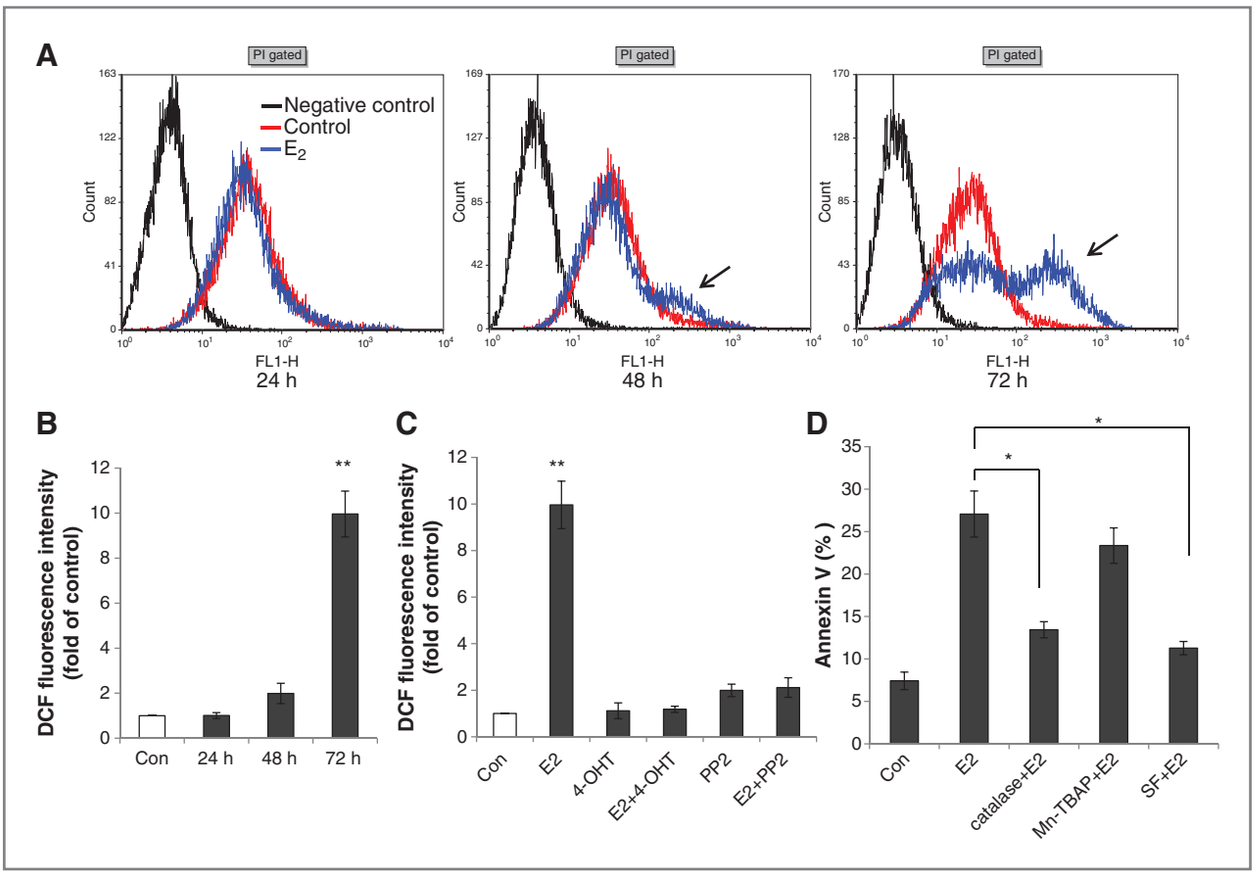

Figure 5. The c-Src inhibitor blocked estrogen-induced oxidative stress in MCF-7:5C cells. A, MCF-7:5C were treated with vehicle and E_2 for different durations. ROS was detected through flow cytometry. B, quantification of ROS production induced by E_2 was compared with control. **, $P < 0.001$, compared with control. C, MCF-7:5C cells were treated with different compounds as above. ROS production was detected through flow cytometry. **, $P < 0.001$, compared with control. D, MCF-7:5C cells were treated with vehicle (0.1% EtOH), E_2 (10^{-9} mol/L), catalase (5,000 U/mL) plus E_2 (10^{-9} mol/L), Mn-TBAP(5×10^{-5} mol/L) plus E_2 (10^{-9} mol/L), sodium formate (2×10^{-3} mol/L) plus E_2 (10^{-9} mol/L) for 72 hours. Apoptosis was detected through Annexin V binding assay. *, $P < 0.05$, compared with E_2-treated group.

in clinical studies (47). After a period of proliferative quiescence lasting a few months, the return of proliferation is similar to the relapses observed 12 to 18 months after primary hormonal therapy in patients. Multiple pathways are involved in the adaptive response to the pressure of E_2 deprivation (48). Although MCF-7 cells grown long-term have been shown to differ substantially in various properties depending upon the number of passages and geographic source of the cell lines, induction of apoptosis by physiologic concentrations of E_2 is the common characteristic of these *in vitro* model systems (20, 21). Nevertheless, how E_2 induces apoptosis is at present unclear. Our new observation (29) that a c-Src inhibitor paradoxically can block E_2-induced apoptosis naturally demands further study. We examined this aspect of c-Src pharmacology to describe fully this phenomenon and gain an insight into the convergence of ER and c-Src pathways for the modulations of an apoptotic trigger in breast cancer. Here, for the first time, we document that c-Src participates in the mediation of stress responses induced by E_2 to widely activate apoptosis-related genes involved in the intrinsic and the extrinsic apoptosis pathways.

The ER is the initial point for E_2 to induce apoptosis, as antiestrogens ICI 182,780 and 4-OHT completely block apoptosis triggered by E_2 (ref. 20 and Supplementary Fig. S3A). Contradictory to the traditional apoptosis mechanism caused by cytotoxic chemotherapy with cell-cycle arrest, E_2-induced apoptotic cells simultaneously undergo proliferation with an increased S-phase of cell cycle resulting in increased cell number despite p53 family members being upregulated (Figs. 1D and 4B). E_2 exerts a dual function on MCF-7:5C cells, with both initial proliferation and the apoptosis. In other words, the initial response of E_2 to stimulate growth is the upregulating of classical transcriptional activity by ER (Fig. 3B) without any detected apoptotic changes in the first 24 hours. Activation of apoptotic genes appeared after 48-hour treatment with E_2 (data not shown) and reached a peak by 72 hours (Fig. 4B–D). Consistently, characteristic apoptosis occurred at 72 hours (Fig. 2A). These data suggest that the higher rate of proliferation by E_2 might activate other pathways to trigger apoptosis. Our data show that E_2 caused endoplasmic reticulum stress, which activated the UPR within 24 hours (Fig. 6A). The initial aim of UPR is to restore normal function of the cell; however, if

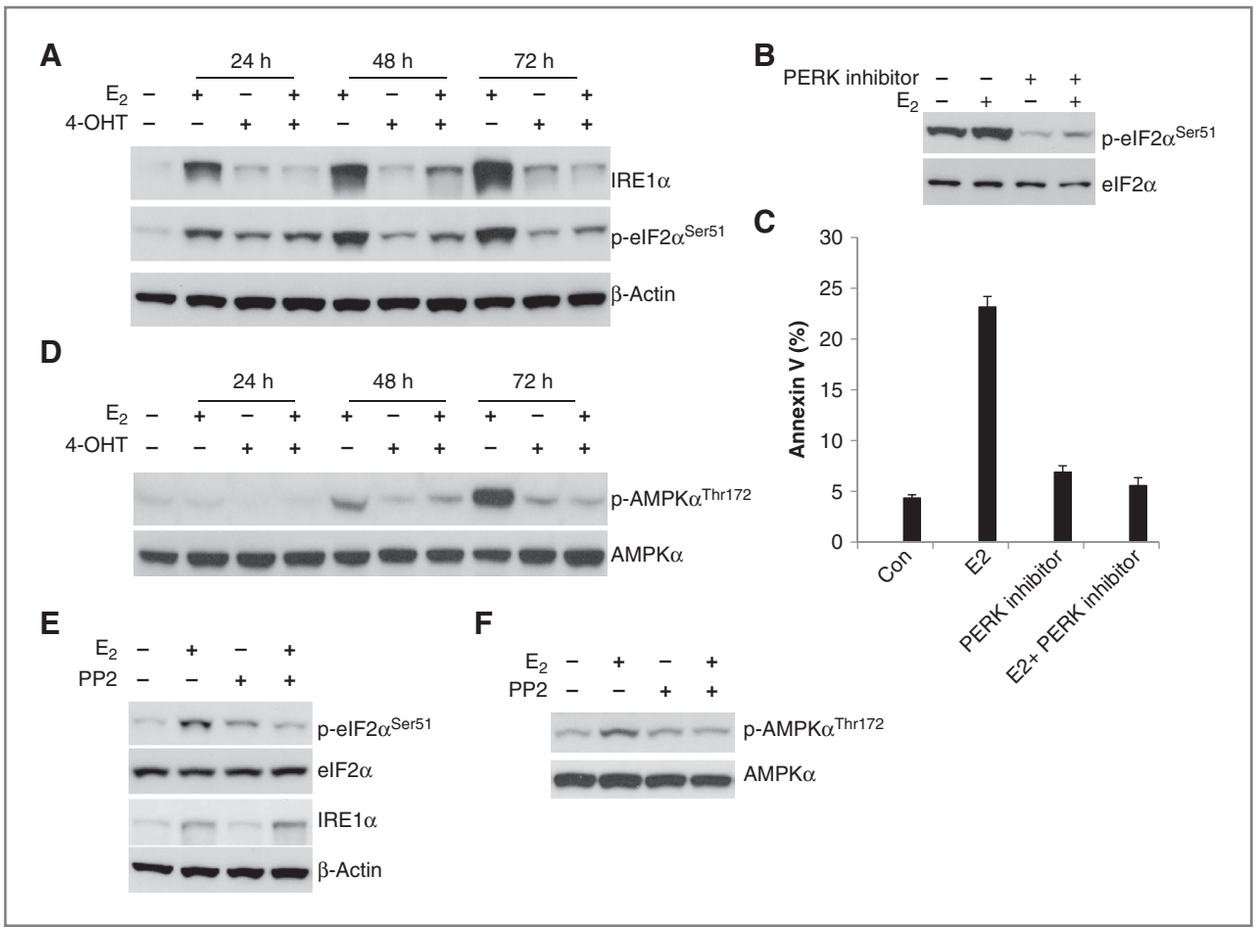

Figure 6. c-Src was involved in estrogen-induced endoplasmic reticulum stress in MCF-7:5C cells. A, MCF-7:5C were treated with E_2 (10^{-9} mol/L) or combined with 4-OHT (10^{-6} mol/L) for different durations. IRE1α and phosphorylated eIF2α were used as indicators of UPR activation. B, MCF-7:5C cells were treated with vehicle (0.1% dimethyl sulfoxide), E_2 (10^{-9} mol/L), PERK inhibitor (1×10^{-5} mol/L), E_2 (10^{-9} mol/L) plus PERK inhibitor (1×10^{-5} mol/L), respectively, for 24 hours. Phosphorylated eIF2α was examined as the downstream of PERK. Total eIF2α was determined for loading control. C, MCF-7:5C cells were treated with E_2 or combined with PERK inhibitor, respectively, for 72 hours. Apoptosis was detected through Annexin V binding assay. D, MCF-7:5C cells were treated with E_2 or combined with 4-OHT as above. Phosphorylated AMPK was examined by immunoblotting. Total AMPK was determined for loading control. E, MCF-7:5C cells were treated with E_2 or combined with PP2 for 24 hours. IRE1α and phosphorylated eIF2α were examined by immunoblotting. Total eIF2α and β-actin were determined for loading controls. F, MCF-7:5C cells were treated with E_2 or combined with PP2 for 48 hours. Phosphorylated AMPK and total AMPK were examined by immunoblotting.

the damage is too severe to repair, the UPR ultimately initiates cell death through activation of the apoptotic pathway (49).

c-Src functioned as an important downstream signal of ER in MCF-7:5C cells, which was activated by E_2 (Fig. 1B, Supplementary Fig. S1A–S1C) and showed multiple levels of association with ER (Figs. 1B and C, 2A, 3A, C, and D). An important finding in this study is that c-Src tyrosine kinase is critical for E_2 -induced apoptosis (Fig. 2A, C, and D). This, therefore, raised the question of the actual role played by c-Src in the process of apoptosis induced by E_2. c-Src mediated PI3K/AKT and MAPK growth pathways by E_2 (Fig. 1C). However, specific inhibitors of PI3K/Akt (LY294002) and MAPK (U0126) could inhibit cell growth but did not prevent E_2-induced apoptosis in MCF-7:5C cells (Supplementary Fig. S7), which imply that MAPK/Akt growth pathways are not directly involved in the apoptosis-induced by E_2. In MCF-7:5C cells, E_2 activated the nongenomic pathway after 10-minute treatment and the c-Src inhibitor blocked the nongenomic pathway (Supplementary Fig. S1A and S1B). Detectable elevation of c-Src phosphorylation appeared after 30-minute treatment with E_2 (Supplementary Fig. S1B). Consistent stimulation of c-Src appeared after 24-hour treatment and gradually increased when extending to 48 hours (Fig. 1B and Supplementary Fig. S1C). All of these data suggest that c-Src activation is a direct effect resulting from E_2. To further explore the function of the nongenomic pathway in the process of E_2-induced apoptosis, EDC was used to treat MCF-7:5C cell, which is very ineffective in stimulating transcription of endogenous E_2 target genes (38). The EDC (10^{-8} mol/L) activated the nongenomic pathway but without capacity to activate genomic pathway and did not induce apoptosis in MCF-7:5C cells (Supplementary Fig. S2). All of these results suggest that the nongenomic pathway does not play a critical role in the E_2-induced apoptosis. Interestingly, the EDC could continuously activate c-Src and Akt but without

any effect on MAPK after 24-hour treatment (Supplementary Fig. S2E), which may be resulted from enhanced association between ERα and membrane growth factor receptor (48).

In addition, E_2 activated classical ERE activity but the c-Src inhibitor could not block the response (Fig. 3B). Furthermore, the c-Src inhibitor collaborated with E_2 to upregulate endogenous ER target genes pS2 and PR (Fig. 3C and D). All of these results imply that classical ER transcriptional pathways are not directly involved in E_2-induced apoptosis. Similarly, Zhang and colleagues reported that the inhibitory effects of E_2 on cell growth are independent of the classical ERE-regulated transcriptional genes (50). Our global gene array data suggest that E_2 signaling can occur through a nonclassical transcriptional pathway involving the interaction of ER with other transcription factors such as activator protein-1 (AP-1) and Sp1, which may regulate stress responses (25). In the present study, E_2 initiated UPR (Fig. 6A), increased ROS production (Fig. 5A), and widely activated apoptosis-related genes (Fig. 4A). The c-Src was involved in the stress responses and inhibition of c-Src decreased the expression of apoptosis-related genes induced by E_2, which are critical mechanisms for the blockade of c-Src to prevent E_2-induced apoptosis.

Overall, E_2 induces endoplasmic reticulum and mitochondrial stresses in MCF-7:5C cells, which subsequently upregulates apoptosis-related genes to activate intrinsic and extrinsic apoptotic pathways. Unexpectedly, c-Src tyrosine kinase plays a critical role in the stress response induced by E_2. These data clearly raise a concern about the ubiquitous use of c-Src inhibitors to treat patients with advanced aromatase inhibitor–resistant breast cancer, thereby undermining the beneficial effects of E_2-induced apoptosis.

Disclosure of Potential Conflicts of Interest

No potential conflicts of interest were disclosed.

Disclaimer

The views and opinions of the author(s) do not reflect those of the U.S. Army or the Department of Defense.

Authors' Contributions

Conception and design: P. Fan, J. Katzenellenbogen, J.W. Gray, V.C. Jordan
Development of methodology: P. Fan, O.L. Griffith, F.A. Agboke, X. Zou, J. Katzenellenbogen, J.W. Gray
Acquisition of data (provided animals, acquired and managed patients, provided facilities, etc.): P. Fan, F.A. Agboke, X. Zou, R.E. McDaniel, K. Creswell, J.W. Gray, V.C. Jordan
Analysis and interpretation of data (e.g., statistical analysis, biostatistics, computational analysis): P. Fan, O.L. Griffith, P. Anur, K. Creswell, J. Katzenellenbogen, J.W. Gray, V.C. Jordan
Writing, review, and/or revision of the manuscript: P. Fan, O.L. Griffith, J. Katzenellenbogen, V.C. Jordan
Administrative, technical, or material support (i.e., reporting or organizing data, constructing databases): O.L. Griffith, R.E. McDaniel, V.C. Jordan
Study supervision: P. Fan, V.C. Jordan
Synthesis of EDC: S.H. Kim

Grant Support

V.C. Jordan is supported by the Department of Defense Breast Program under Award number W81XWH-06-1-0590 Center of Excellence; subcontract under the SU2C (AACR) Grant number SU2C-AACR-DT0409; the Susan G Komen For The Cure Foundation under Award number SAC100009; GHUCCTS CTSA (Grant # UL1RR031975); and the Lombardi Comprehensive Cancer Center Support Grant (CCSG) Core Grant NIH P30 CA051008. J.W. Gray is supported by a Stand Up to Cancer Dream Team Translational Cancer Research Grant, a Program of the Entertainment Industry Foundation (SU2C-AACR-DT0409). J. Katzenellenbogen is supported by NIH grant (PHS 5R37DK015556). O.L. Griffith was supported by a fellowship from the Canadian Institutes of Health Research (CIHR).

The costs of publication of this article were defrayed in part by the payment of page charges. This article must therefore be hereby marked *advertisement* in accordance with 18 U.S.C. Section 1734 solely to indicate this fact.

Received November 8, 2012; revised March 22, 2013; accepted April 22, 2013; published OnlineFirst May 23, 2013.

References

1. Jordan VC. A century of deciphering the control mechanisms of sex steroid action in breast and prostate cancer: the origins of targeted therapy and chemoprevention. Cancer Res 2009;69:1243–54.
2. Jordan VC, Brodie AM. Development and evolution of therapies targeted to the estrogen receptor for the treatment and prevention of breast cancer. Steroids 2007;72:7–25.
3. Sabnis G, Schayowitz A, Goloubeva O, Macedo L, Brodie A. Trastuzumab reverses letrozole resistance and amplifies the sensitivity of breast cancer cells to estrogen. Cancer Res 2009;69:1416–28.
4. Jordan VC, O'Malley BW. Selective estrogen-receptor modulators and antihormonal resistance in breast cancer. J Clin Oncol 2007;25:5815–24.
5. Massarweh S, Osborne CK, Creighton CJ, Qin L, Tsimelzon A, Huang S, et al. Tamoxifen resistance in breast tumors is driven by growth factor receptor signaling with repression of classic estrogen receptor genomic function. Cancer Res 2008;68:826–33.
6. Sabnis G, Goloubeva O, Jelovac D, Schayowitz A, Brodie A. Inhibition of the phosphatidylinositol 3-kinase/Akt pathway improves response of long-term estrogen-deprived breast cancer xenografts to antiestrogens. Clin Cancer Res 2007;13:2751–7.
7. McKenna NJ, O'Malley BW. Combinatorial control of gene expression by nuclear receptors and coregulators. Cell 2002;108:465–74.
8. Yao K, Lee ES, Bentrem DJ, England G, Schafer JI, O'Regan RM, et al. Antitumor action of physiological estradiol on tamoxifen-stimulated breast tumors grown in athymic mice. Clin Cancer Res 2000;6:2028–36.
9. Osipo C, Gajdos C, Liu H, Chen B, Jordan VC. Paradoxical action of fulvestrant in estradiol-induced regression of tamoxifen-stimulated breast cancer. J Natl Cancer Inst 2003;95:1597–608.
10. Liu H, Lee ES, Gajdos C, Pearce ST, Chen B, Osipo C, et al. Apoptotic action of 17beta-estradiol in raloxifene-resistant MCF-7 cells *in vitro* and *in vivo*. J Natl Cancer Inst 2003;95:1586–97.
11. Ellis MJ, Gao F, Dehdashti F, Jeff DB, Marcom PK, Carey LA, et al. Lower-dose vs high-dose oral estradiol therapy of hormone receptor-positive, aromatase inhibitor-resistant advanced breast cancer: a phase 2 randomized study. JAMA 2009;302:774–80.
12. Anderson GL, Chlebowski RT, Aragaki AK, Kuller LH, Manson JE, Gass M, et al. Conjugated equine oestrogen and breast cancer incidence and mortality in postmenopausal women with hysterectomy: extended follow-up of the Women's Health Initiative randomised placebo-controlled trial. Lancet Oncol 2012;13:476–86.
13. Obiorah I, Jordan VC. The scientific rationale for a delay after menopause in the use of conjugated equine estrogens in postmenopausal women that causes a reduction in breast cancer incidence and mortality. Menopause 2013;20:372–82.
14. Thomas SM, Brugge JS. Cellular functions regulated by Src family kinases. Ann Rev Cell Dev Biol 1997;13:513–609.
15. Pascoe D, Oursler MJ. The Src signaling pathway regulates osteoclast lysosomal enzyme secretion and is rapidly modulated by estrogen. J Bone Miner Res 2001;16:1028–36.
16. Jallal H, Valentino ML, Chen G, Boschelli F, Ali S, Rabbani SA. A Src/Abl Kinase inhibitor, SKI-606, blocks breast cancer invasion, growth, and metastasis *in vitro* and *in vivo*. Cancer Res 2007;67:1580–8.
17. Fan P, Wang J, Santen RJ, Yue W. Long-term treatment with tamoxifen facilitates translocation of estrogen receptor alpha out of the nucleus and enhances its interaction with EGFR in MCF-7 breast cancer cells. Cancer Res 2007;67:1352–60.

18. Hiscox S, Jordan NJ, Smith C, James M, Morgan L, Taylor KM, et al. Dual targeting of SRC and ER prevents acquired antihormone resistance in breast cancer cells. Breast Cancer Res Treat 2009;115:57–67.
19. Green DR, Reed JC. Mitochondria and apoptosis. Science 1998;281:1309–12.
20. Lewis JS, Meeke K, Osipo C, Ross EA, Kidawi N, Li T, et al. Intrinsic mechanism of estradiol-induced apoptosis in breast cancer cells resistant to estrogen deprivation. J Natl Cancer Inst 2005;97:1746–59.
21. Song RX, Mor G, Naftolin F, McPherson RA, Song J, Zhang Z, et al. Effect of long-term estrogen deprivation on apoptotic responses of breast cancer cells to 17 beta-estradiol. J Natl Cancer Inst 2001;93:1714–23.
22. Green DR, Kroemer G. The pathophysiology of mitochondrial cell death. Science 2004;305:626–9.
23. Balaban RS, Nemoto S, Finkel T. Mitochondria, oxidants, and aging. Cell 2005;120:483–95.
24. Ferri KF, Kroemer G. Organelle-specific initiation of cell death pathways. Nat Cell Biol 2001;3:E255–63.
25. Ariazi EA, Cunliffe HE, Lewis-Wambi JS, Slifker MJ, Willis AL, Ramos P, et al. Estrogen induces apoptosis in estrogen deprivation-resistant breast cancer through stress responses as identified by global gene expression across time. Proc Natl Acad Sci USA 2011;108:18879–86.
26. Chakrabarti A, Chen AW, Varner JD. A review of the mammalian unfolded protein response. Biotechnol Bioeng 2011;108:2777–93.
27. Tsai YC, Weissman AM. The unfolded protein response, degradation from endoplasmic reticulum and cancer. Genes Cancer 2010;1:764–78.
28. Roberts CG, Gurisik E, Biden TJ, Sutherland RL, Butt AJ. Synergistic cytotoxicity between tamoxifen and the plant toxin persin in human breast cancer cells is dependent on Bim expression and mediated by modulation of ceramide metabolism. Mol Cancer Ther 2007;6:2777–85.
29. Fan P, McDaniel RE, Kim HR, Clagett D, Haddad B, Jordan VC. Modulating therapeutic effects of the c-Src inhibitor via oestrogen receptor and human epidermal growth factor receptor 2 in breast cancer cell lines. Eur J Cancer 2012;48:3488–98.
30. Tobaben S, Grohm J, Seiler A, Conrad M, Plesnila N, Culmsee C. Bid-mediated mitochondrial damage is a key mechanism in glutamate-induced oxidative stress and AIF-dependent cell death in immortalized HT-22 hippocampal neurons. Cell Death Differ 2011;18:282–92.
31. Trapnell C, Pachter L, Salzberg SL. TopHat: discovering splice junctions with RNA-seq. Bioinformatics 2009;25:1105–11.
32. Trapnell C, Williams BA, Pertea G, Mortazavi A, Kwan G, Baren MJ, et al. Transcript assembly and quantification by RNA-seq reveals unannotated transcripts and isoform switching during cell differentiation. Nat Biotechnol 2010;28:511–5.
33. Griffith M, Griffith OL, Mwenifumbo J, Goya R, Morrissy AS, Morin RD, et al. Alternative expression analysis by RNA sequencing. Nat Methods 2010;7:843–7.
34. Huang da W, Sherman BT, Lempicki RA. Systematic and integrative analysis of large gene lists using DAVID Bioinformatics Resources. Nat Protoc 2009;4:44–57.
35. Fan P, Yue W, Wang JP, Aiyar S, Li Y, Kim TH, et al. Mechanisms of resistance to structurally diverse antiestrogens differ under premenopausal and postmenopausal conditions: evidence from *in vitro* breast cancer cell models. Endocrinology 2009;150:2036–45.
36. Kousteni S, Bellido T, Plotkin LI, O'Brien CA, Bodenner DL, Han L, et al. Nongenotropic, sex-onspecific signaling through the estrogen or androgen receptors: dissociation from transcriptional activity. Cell 2001;104:719–30.
37. Shupnik MA. Crosstalk between steroid receptors and the c-Src-receptor tyrosine kinase pathways: implications for cell proliferation. Oncogene 2004;23:7979–89.
38. Harrington WR, Kim SH, Funk CC, Madak-Erdogan Z, Schiff R, Katzenellenbogen JA, et al. Estrogen dendrimer conjugates that preferentially activate extranuclear, nongenomic versus genomic pathways of estrogen action. Mol Endocrinol 2006;20:491–502.
39. Chu I, Arnaout A, Loiseau S, Sun J, Seth A, McMahon C, et al. Src promotes estrogen-dependent estrogen receptor alpha proteolysis in human breast cancer. J Clin Invest 2007;117:2205–15.
40. Araujo JA, Zhang M, Yin F. Heme oxygenase-1, oxidation, inflammation, and atherosclerosis. Front Pharmacol 2012;3:119.
41. Nishikawa T, Edelstein D, Du XL, Yamagishi S, Matsumura T, Kaneda Y, et al. Normalizing mitochondrial superoxide production blocks three pathways of hyperglycaemic damage. Nature 2000;404:787–90.
42. Matsuda S, Umeda M, Uchida H, Kato H, Araki T. Alterations of oxidative stress markers and apoptosis markers in the striatum after transient focal cerebral ischemia in rats. J Neural Transm 2009;116:395–404.
43. Harding HP, Zhang Y, Zeng H, Novoa I, Lu PD, Calfon M, et al. An integrated stress response regulates amino acid metabolism and resistance to oxidative stress. Mol Cell 2003;11:619–33.
44. Dagon Y, Avraham Y, Berry EM. AMPK activation regulates apoptosis, adipogenesis, and lipolysis by eIF2*a* in adipocytes. Biochem Biophys Res Commun 2006;340:43–7.
45. Birnbaum MJ. Activating AMP-activated protein kinase without AMP. Mol Cell 2005;19:289–90.
46. Sweeney EE, McDaniel RE, Maximov PY, Fan P, Jordan VC. Models and mechanisms of acquired antihormone resistance in breast cancer: significant clinical progress despite limitations. Horm Mol Biol Clin Investig 2012;9:143–63.
47. Jiang SY, Wolf DM, Yingling JM, Chang C, Jordan VC. An estrogen receptor positive MCF-7 clone that is resistant to antiestrogens and estradiol. Mol Cell Endocrinol 1992;90:77–86.
48. Santen RJ, Song RX, Zhang Z, Kumar R, Jeng MH, Masamura S, et al. Adaptive hypersensitivity to estrogen: Mechanisms and clinical relevance to aromatase inhibitor therapy in breast cancer treatment. J Steroid Biochem Mol Biol 2005;95:155–65.
49. Nakagawa T, Zhu H, Morishima N, Li E, Xu J, Yankner BA, et al. Caspase-12 mediates endoplasmic-reticulum-specific apoptosis and cytotoxicity by amyloid-beta. Nature 2000;403:98–103.
50. Zhang Y, Zhao H, Asztalos S, Chisamore M, Sitabkhan Y, Tonetti DA. Estradiol-induced regression in T47D:A18/PKCalpha tumors requires the estrogen receptor and interaction with the extracellular matrix. Mol Cancer Res 2009;7:498–510.